Finite Element Analysis of the SPIRE structure **SPIRE-MSS-PRJ-001141**

Glossary

All terms are listed in the CIDL.

Documents

All documents are listed in Figure 3.2 of the CIDL.

1. Introduction

This document describes the Finite Element Model of the SPIRE structure and lists its main properties. Furthermore analysis results are given in the appendices. The structure of the document is as follows.

1) Rough outline of the model, providing background information and main purpose of the model.
2) Type of elements used.
3) Static properties of the model.
4) Dynamic properties of the model.
5) Requirements on dynamic behaviour of the model and notching for sine and random vibration.
6) Notch predicitions
7) Load generation and load definition for subsystems.(next issue, currently reported in several small technotes)
8) Appendices:
    response plots sine
    response plots random
    response correlation (during tests only a limited number of responses can be monitored

The model used in the analysis is issue 8. The previous models (issues) have not been reported in much detail, they were used for sizing and estimating loads for the system and subsystems. This is the first report to wrap up the main characteristics of the structure and provides for a configuration controlled reference from now on. The issue 8 FEM version of the structure was built in September 2001. Since then several changes have been implemented in the design of the structure that are not reflected in issue 8 of the FEM.

2. Outline of the model

The model used in the analysis was created by hand, no automatic meshing procedures/routines have been used. It was created in issue 8m2 of SDRC Ideas. Since the SPIRE structure consists mainly of shell like elements (apart of the smaller subsystems and the mirror mounts) primarily beam and shell elements were used for this model. A few rigid, spring and lumped mass elements were used. The amount of rigid elements was kept to an absolute minimum and were only implemented with zero-length. This in order not to introduce unrealistic strains due to thermal deformation. All spring elements used in this model also have zero length. This in order not to introduce phantom forces or moments. Figure 1 gives the geometry of the design and figure 2 the FEM representation.

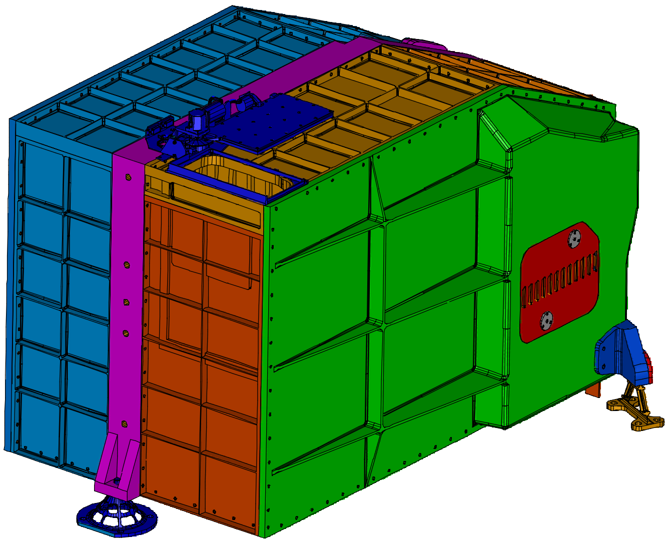

Figure 1: Geometry of the SPIRE structure

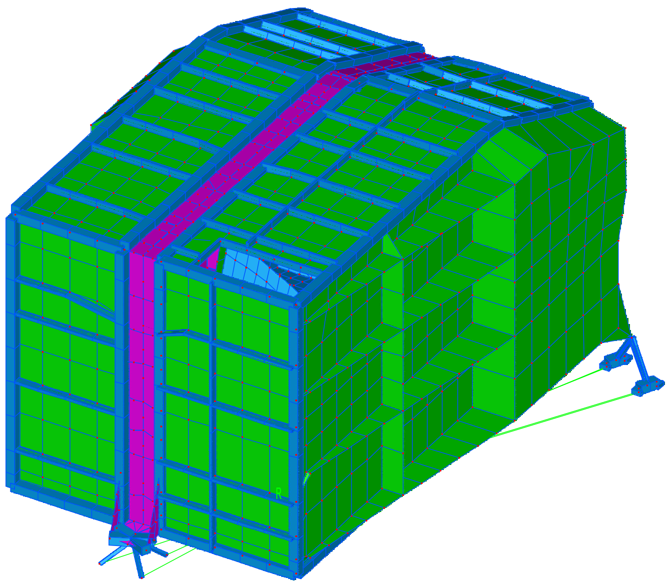

Figure 2: FEM of the SPIRE structure

Comparing both figures it can be readily seen that several details have been ignored or modelled in a simple way. A few examples. Near the entry of the instrument all details of the shutter have been ignored, only the mass of it is represented in the model. The same has been done for most subsystems. Sometimes the geometry has been mimicked in order to have a more realistic mass distribution. Only in the case of the detectors the stiffness has been modelled in order to have a more realistic (local) response. The reason for this is that the detectors have eigenfrequencies in the range of 200 to 300 Hz. Which is close to the instrument main structure modes (between 130 and 200 Hz) For all other subsystems the eigenfrequencies are well above 400 Hz. All mirrors and mirrors mounts have eigenfrequencies above 800 Hz (most of them well above 1500 Hz). So it was judged that they could be represented by lumped masses or relatively thick shell elements. The instrument structure consists of the following parts. A monocoque shell holding and an optical bench. The mono-coque shell itself is statically determined suspended of the spacecraft optical bench. The instrument optical bench carries all the parts that make up a spectrometer (on the +y side of the optical bench) and a photometer (on the -Y side of the optical bench)

The photometer side of the optical bench (as modelled in the FEM) is shown in figure 3.

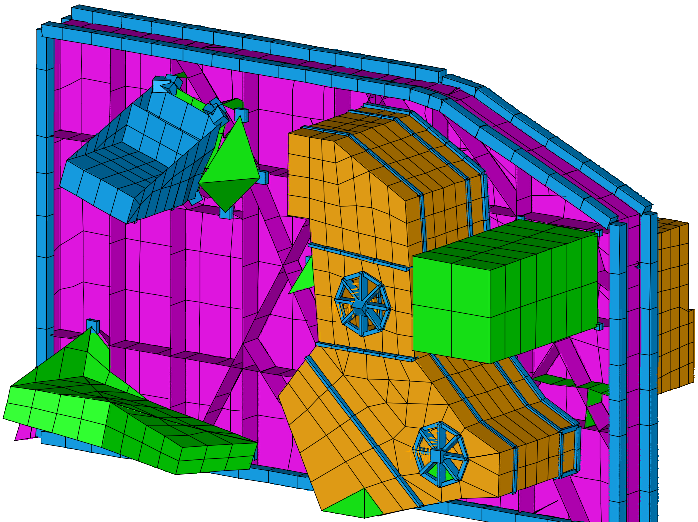

Figure 3: The instrument optical bench (photometer side) FEM

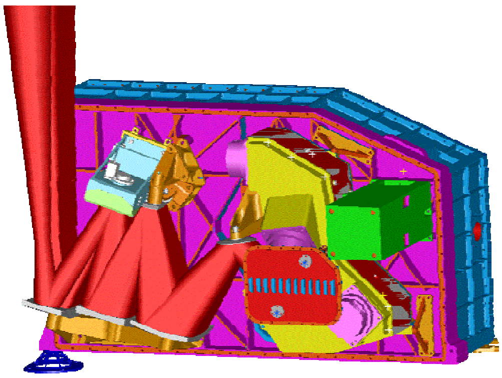

Figure 4: The instrument optical bench (photometer side) real design

The large orange box is the photometer detector box, carrying 3 detectors. On the photometer side the He fridge is mounted (visible as the green box top right-hand side). The secondary optical bench in the bottom left corner (green) with the three mirrors as lumped masses. The beam steering mirror mechanism is visible as a blue structure in the top left corner. Other mirror mounts are triangular elements ending at the mounting location of the mirror (modelled as lumped masses)

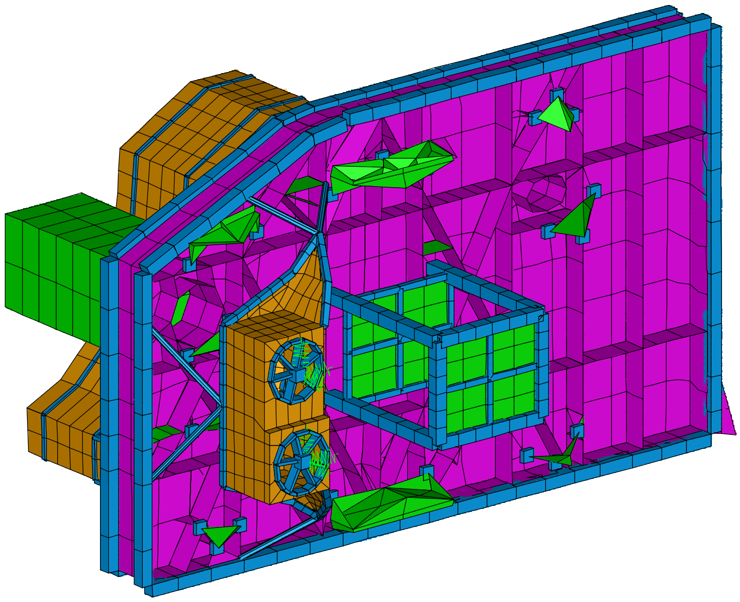

Figure 5: The instrument optical bench (spectrometer side) FEM

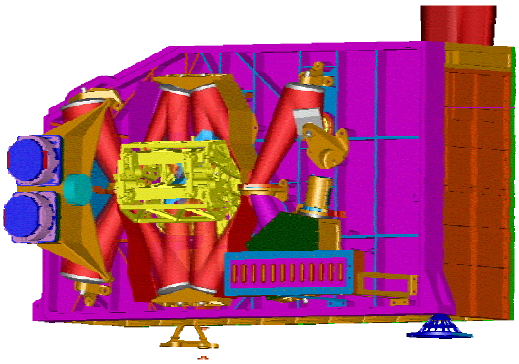

Figure 6: The instrument optical bench (spectrometer side) real design

The spectrometer side of the optical bench shows the detector box with the two detectors. The SMEC-m (spectrometer mechanism) is represented only for its mass. Its mass is distributed using beam and shell elements. The mirror and mirror mounts are modelled using lumped masses and triangular elements.

The interface on which the instrument is mounted is assumed to be infinetly stiff and modelled as such. For convenience an extra grid is introduced below the instrument. From this grid a rigid element is connected to all intereface points of the instrument. This element is not part of the model and only used to 'hold' the model in a convenient way.

Some statistics:

```
NUMBER OF NODES      :    3744
NUMBER OF ELEMENTS   :    4254
NUMBER OF EQUATIONS  =    22290 (dof)
```

3. Element types used and co-ordinate system

The element types used are:

Beam (linear)	stiffeners
Rod (linear)	instrument and detector box support
Shell (linear and quadratic)	instrument covers
Springs	tuned local stiffness (detectors) all zero-length
Lumped masses	used for stiff local subsystems and detector modal mass

All analysis results are reported in the global co-ordinate system of the model, unless specified otherwise. The global FEA co-ordinate system is co-aligned with the S/C co-ordinate system. That is:

Launch direction is X
Sun pointing is Z
The other one must be Y

Co-ordinate system is orthogonal and right handed.

The optical bench of the SPIRE instrument is in the X-Z plane. The entry beam of the instrument is pointing (roughly) in the +X-direction which is out of plane for the Herschel optical bench.

4. Static properties

The following properties are for the instrument mounted on an infinite stiff interface. Coordinate system is always the global which is co-aligned with the S/C coordinate system.

Mass 42.34 kg (mass of the FEM, worst case assumption of real instrument mass at the time of the creation of the model)

Ixx	Iyy	Izz
2.494	2.570	1.335
Ixy	Iyz	Izx
-46.57	84.96	67.22

4.1: MoI (around CoG SI units valid for the FEM only)

loadcase	X [g]	Y [g]	Z [g]
1	20	2	-
2	20	-	2
3	-	14	-
4	-	-	14

4.2: Static load definition (IID-A) (and all permutations with pos. or neg. direction)

I/F force direction	[N]	4-sigma [N]
Fx	8307	2077
Fy	5815	1454
Fz	5815	1454

4.3: Static I/F loads (overall)

The 4-sigma equivalent quasi-static is given for comparisson witht the random vibration interface loads.

Worst case interface bolt load due to above specified static load cases (table 4.2)

Pull-out 1750 N (case 4)
Shear 2336 N (case 4)

The worst case interface load is for the cone in the Z-direction. Due to the stiffness distribution the cone is carrying most of the interface load. Assuming the load will be taken by an M6 interface bolt the margin of saftey on pull-out is 3.1 and 0.5 for shear (this is including 1.5 load factor on ultimate or 1.1 load factor on yield)

5. Dynamic Characteristics

The following table lists all eigenfrequencies and modal characteristics between 0 and 300 Hz. The software doesn't list the rotational effective mass.

Mode	Frequency	Stiffness	Modal	Effective mass normalised to unity		
#	[Hz]	[N/m]	Mass [kg]	X	Y	Z
1	135.7	104879	0.143	0.00	**0.75**	0.01
2	151.3	226109	0.249	0.05	0.01	**0.79**
3	189.0	50250	0.035	**0.46**	0.00	0.02
4	191.3	5744	0.012	0.06	0.00	0.03
5	207.4	8039	0.015	0.01	0.01	0.00
6	221.2	54234	0.088	0.05	0.00	0.00
7	226.7	8713	0.013	**0.16**	0.01	0.05
8	237.8	2216	0.003	0.01	0.01	0.00
9	241.7	11930	0.016	0.02	0.00	0.00
10	246.5	16595	0.022	0.00	0.00	0.00
11	255.3	2658	0.003	0.01	0.01	0.00
12	258.0	742	0.001	0.00	0.00	0.00
13	262.1	99	0.000	0.00	0.00	0.00
14	263.1	9326	0.011	0.01	0.00	0.00
15	264.2	1715	0.002	0.00	0.00	0.00
16	265.4	322	0.000	0.01	0.00	0.00
17	273.7	1867	0.002	0.04	0.00	0.00
18	278.8	42654	0.044	0.00	0.00	0.02
19	285.2	17951	0.018	0.01	0.02	0.01
20	292.4	2257	0.002	0.00	0.00	0.00
21	298.7	3739	0.003	0.04	0.00	0.00
			total:	0.93	0.83	0.94

6. Interface Force (sine)

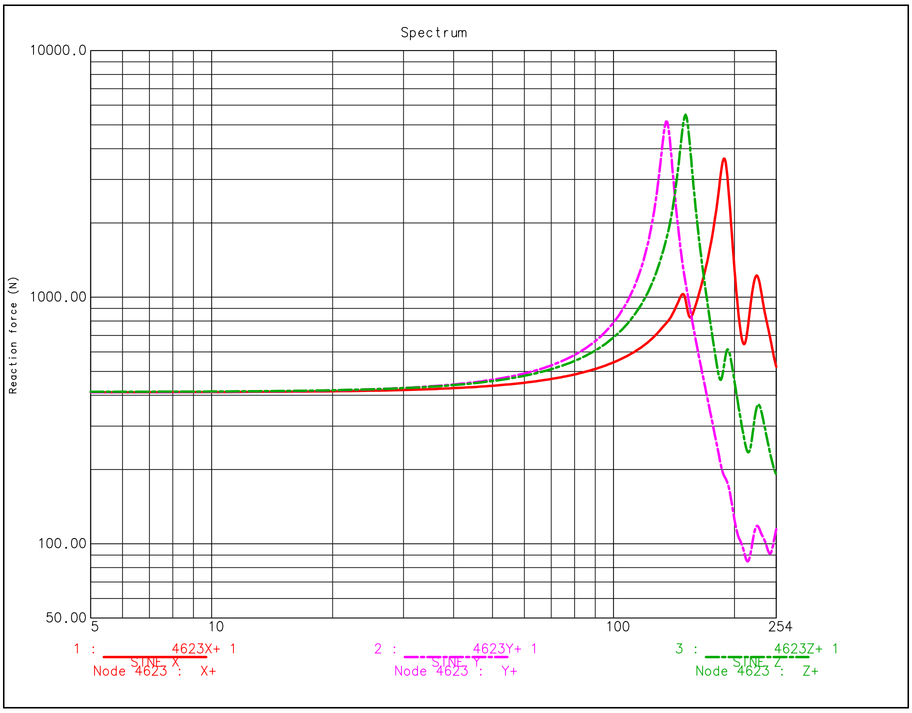

Figure 6.1: Interface forces due to 1 g base acceleration

In figure 6.1 the interface forces in the excitation direction are shown for a 1 g base acceleration. The shown interface force is the algebraic sum of all interface forces. Based upon this interface force and the requirement that the interface force will not exceed equivalent quasi-static forces (see table 4.3) the following input was generated.

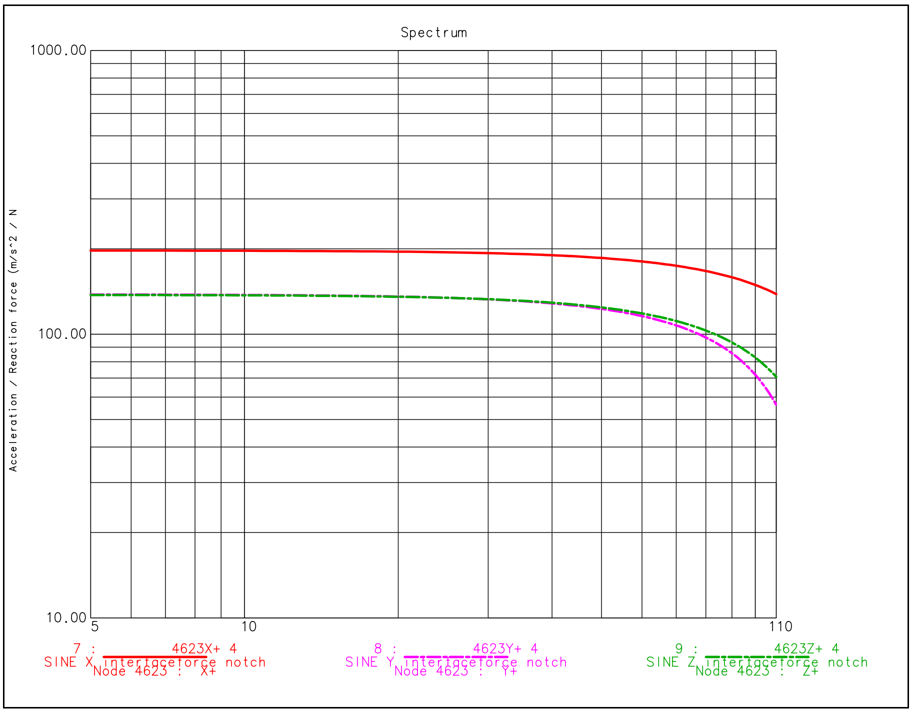

6.2: Sine vibration input for the analysis.
(capped by 20 g in X and 14 g in Y or Z direction)

7. Sine responses (general)

The sine input as specified in figure 6.2 is based upon a 20 g input in X-direction and a 14 g input in either Y or Z direction and then notched on the interface forces taken from table 4.3. The IID-A specifies for the X direction a decrease in input above 40 Hz down to 10 g. Since the instrument has its first mode at about 135 Hz and 150 Hz the resulting input at 100 Hz is capped by the resonances in Y and Z down to 7 and 8.5 g respectively. The first serious X resonance is too high to cause the input to be capped at 100 Hz in the X-direction. In order to take into account a 10% uncertainty in the frequency prediction the sine analysis has been extended to 110 Hz.

Ball park one can assume that the amplification inside the instrument below 110 Hz is lower than a factor of 3-4 since 110 Hz is still sufficiently far away from the first resonance. For the X-direction excitation the amplification will be less than 2 at 110 Hz. This disregarding the actual applied damping, which has no significant influence below 80% (in frequency) of the first resonance).

As a result of the above and taking into account a analysis and design uncertainty factor of 1.5 into account the following sine responses are enveloping all instrument structure responses. That is all structure but the sub-systems. These values can be used as sizing loads for subsystem design if the orientation of the sub-system is known. They are the qualification loads for the sub-systems unless otherwise specified in the mechanucal interface document.

Direction:	X	Y	Z
Sizing input:	30 g all components	30 g for SOB mounted components 45 g for all others	30 g all components

7.1 Enveloping sine responses

Direction (sine input)	Worst case displacement of harness or thermal strap interface in mm
X	< 0.01
Y	< 0.2
Z	<0.15

7.2 Enveloping sine displacements

8. Interface Forces (random)

As for the sine vibration input the input for random vibration is notched based upon equivalent quasi static accelerations. At (clearly defined) resonances the input is decreased in order to scale the 4-sigma random vibration interface load to their quasi-static equivalent counterparts. See table 4.3. The input (pre-scaled to accommodate the notches) is given in figure 8.1. The red line gives the un-notched spectrum (same for all directions, see IID-A).

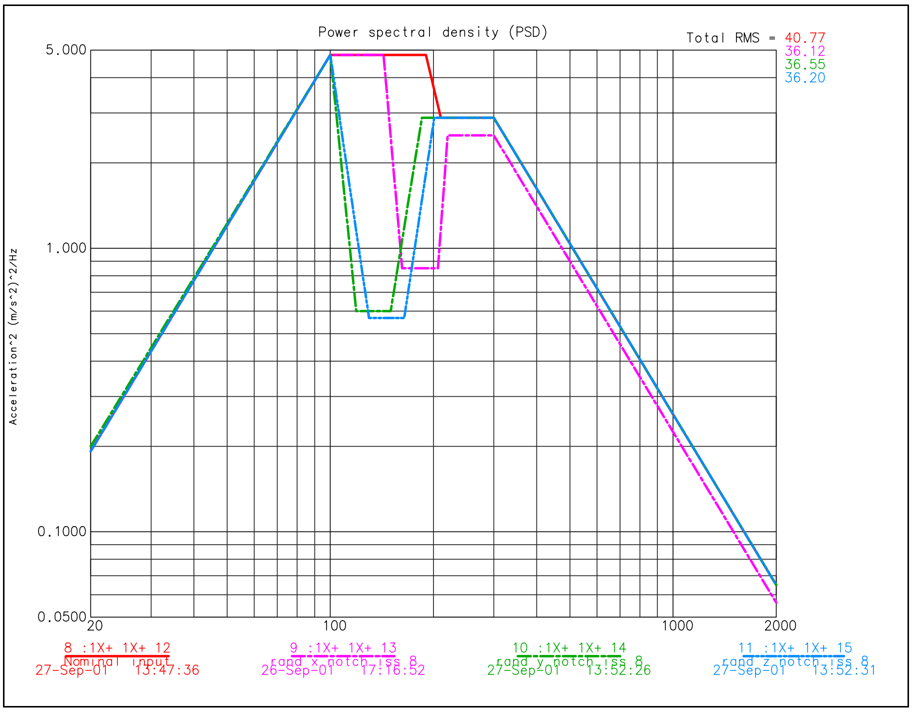

8.1: Un-notched and notched spectra for random vibration

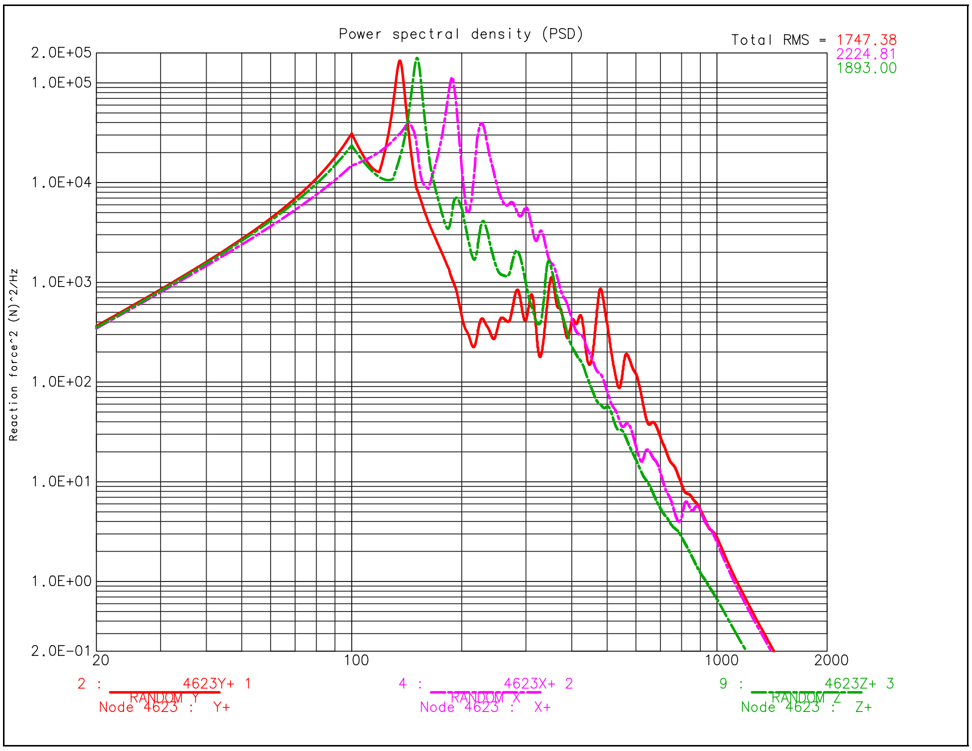

8.2: Resulting interface forces from input as defined in 8.1

The rms-interface forces still exceed the equivalent 4-sigma static interface forces by 10 to 20%.

9. Random vibration responses

The responses of the individual components are not as easily enveloped as for the sine case. This is due to the fact that the random vibration bandwidth includes all major structural modes and also all major sub-system interfaces.

Direction (sine input)	Worst case displacement of harness or thermal strap interface in rms-mm (4-sigma)
X	< 0.01
Y	< 0.05
Z	<0.05

9.1 Random displacements of the structure

10. Thermal Deformation

Apart from its suspension (both instrument and detector boxes) all components are made of aluminium (6082-T6). The support elements for the overall instrument vary slightly in height. For this reason the instrument is tilted slightly around the Y-axis at the cone support. The angel of rotation is less than 0.15 arcmin. Cooled down to less than 10 K the instrument will be compliant with the optical design.

The overall thermal contraction of the instrument with regard to its interface is about 3.5 mm. If the interface doesn't contract at the same rate as the instrument some thermal stress will be induced in the A-frame supports. In order not to exceed any yield stress levels the temperature difference between the interface (if aluminium 6000-series) and the instrument should not exceed 5 K above 100 K.

A. Modeshapes 1 to 9

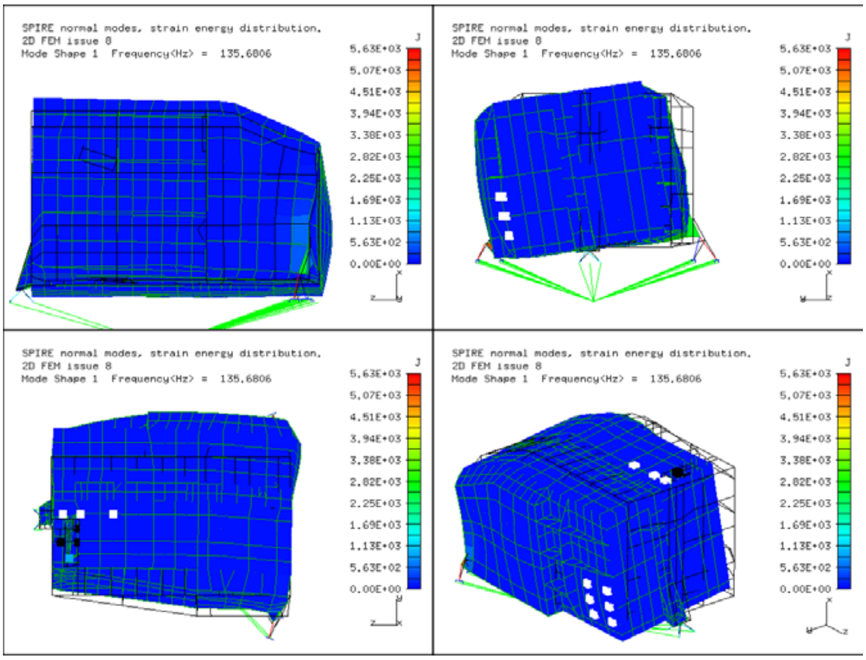

Mode 1: 136 Hz (Y-direction)

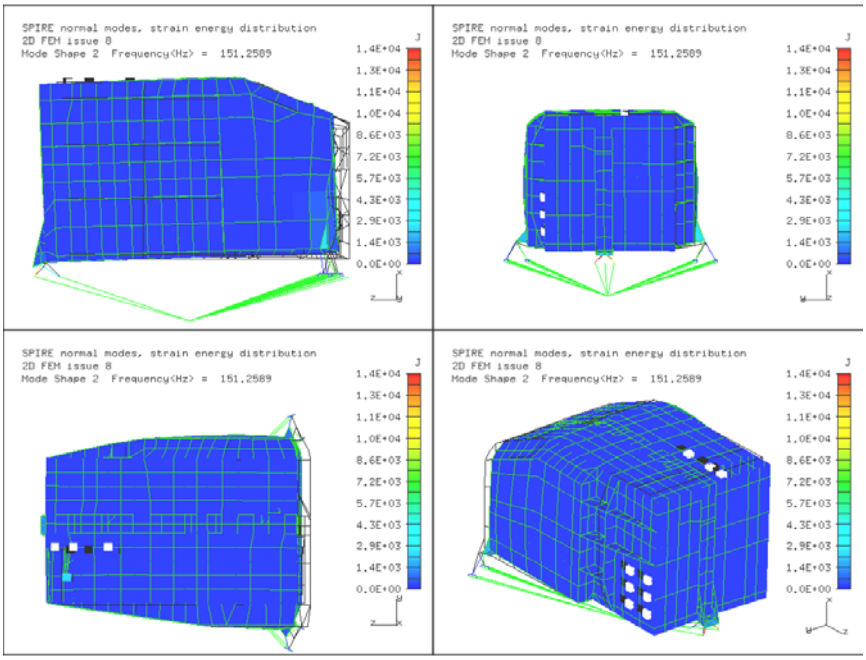

Mode 2: 151 Hz (Z-direction)

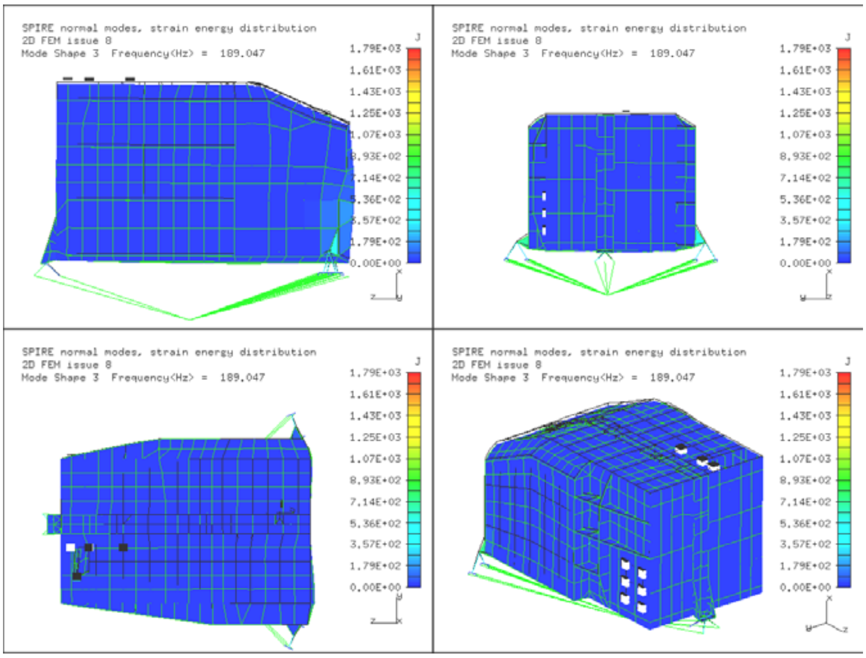

Mode3: 191 Hz (Z-direction)

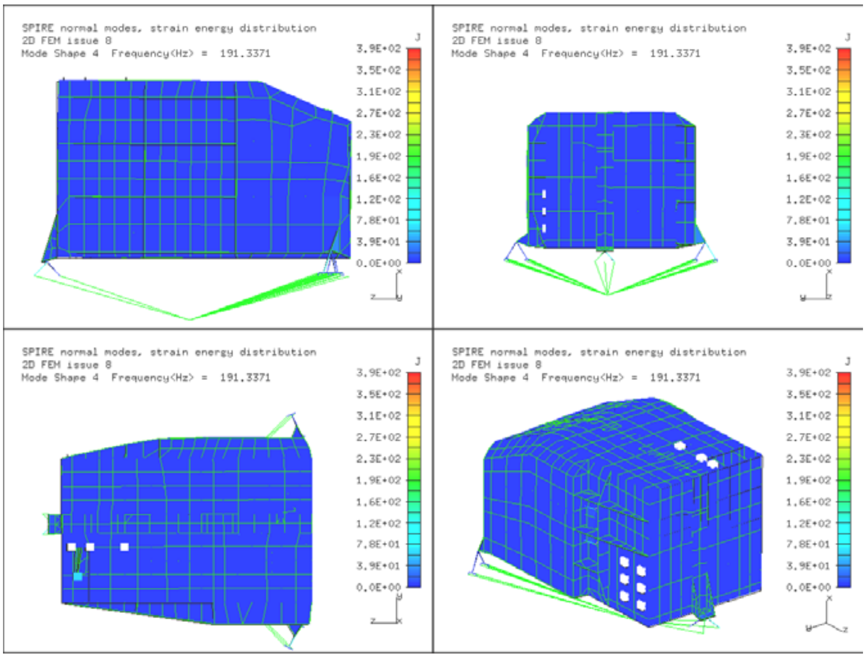

Mode 4

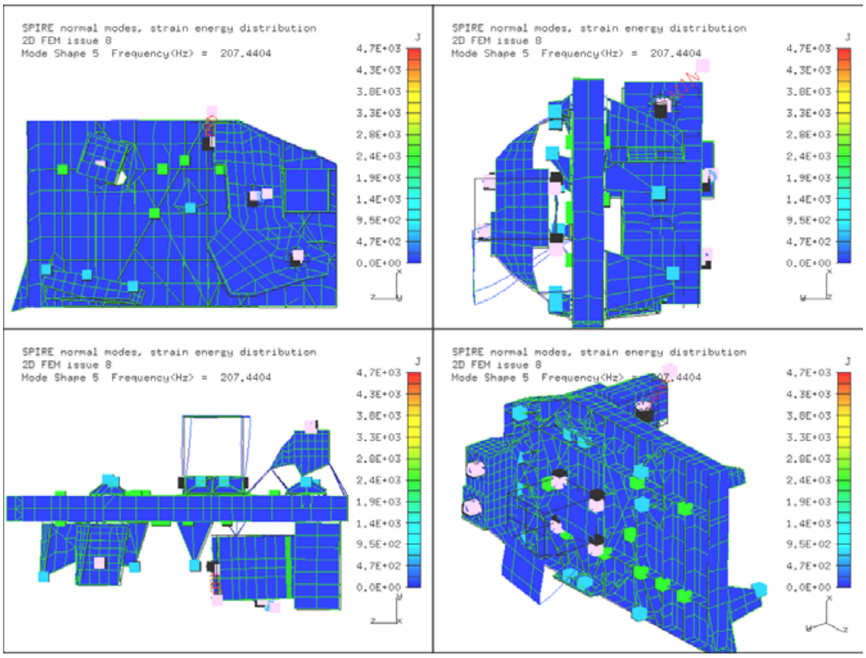
SPIRE normal modes, strain energy distribution
2D FEM issue 8
Mode Shape 5 Frequency(Hz) = 207.4404
J
4.7E+03
4.3E+03
3.8E+03
3.3E+03
2.8E+03
2.4E+03
1.9E+03
1.4E+03
9.5E+02
4.7E+02
0.0E+00

Mode 5

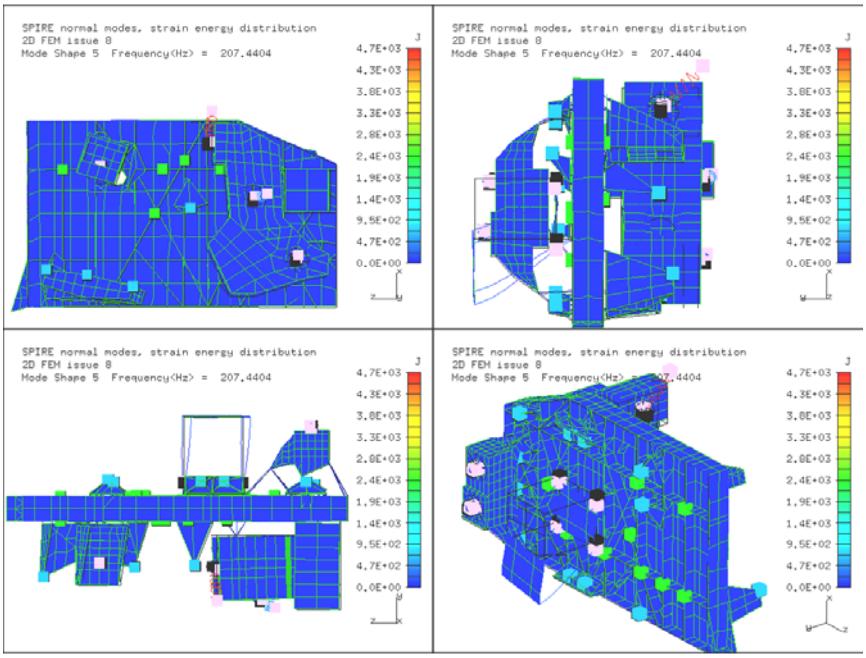
SPIRE normal modes, strain energy distribution
2D FEM issue 8
Mode Shape 5 Frequency(Hz) = 207.4404
J
4.7E+03
4.3E+03
3.8E+03
3.3E+03
2.8E+03
2.4E+03
1.9E+03
1.4E+03
9.5E+02
4.7E+02
0.0E+00

Mode 5

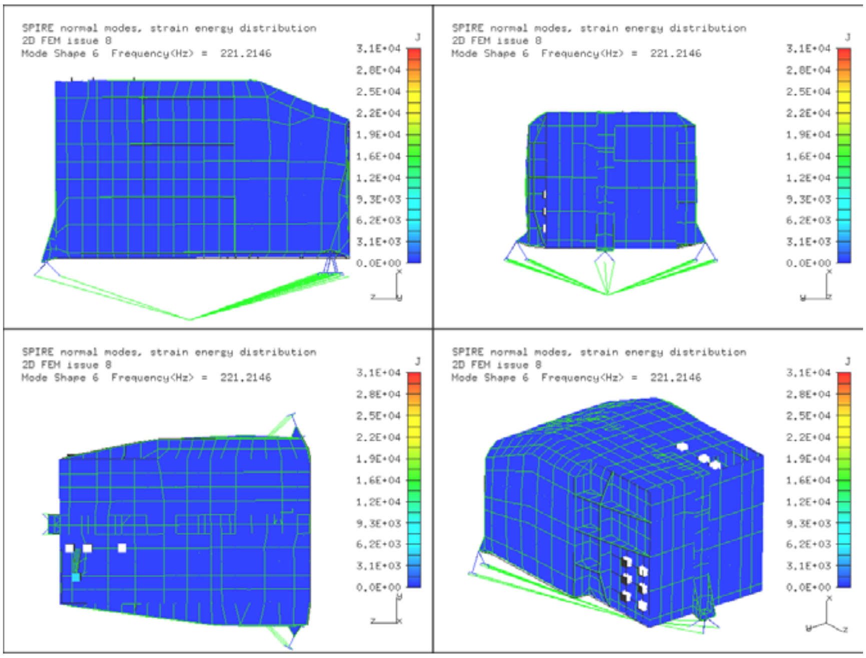
SPIRE normal modes, strain energy distribution
2D FEM issue 8
Mode Shape 6 Frequency(Hz) = 221.2146
J
3.1E+04
2.8E+04
2.5E+04
2.2E+04
1.9E+04
1.6E+04
1.2E+04
9.3E+03
6.2E+03
3.1E+03
0.0E+00

Mode 6

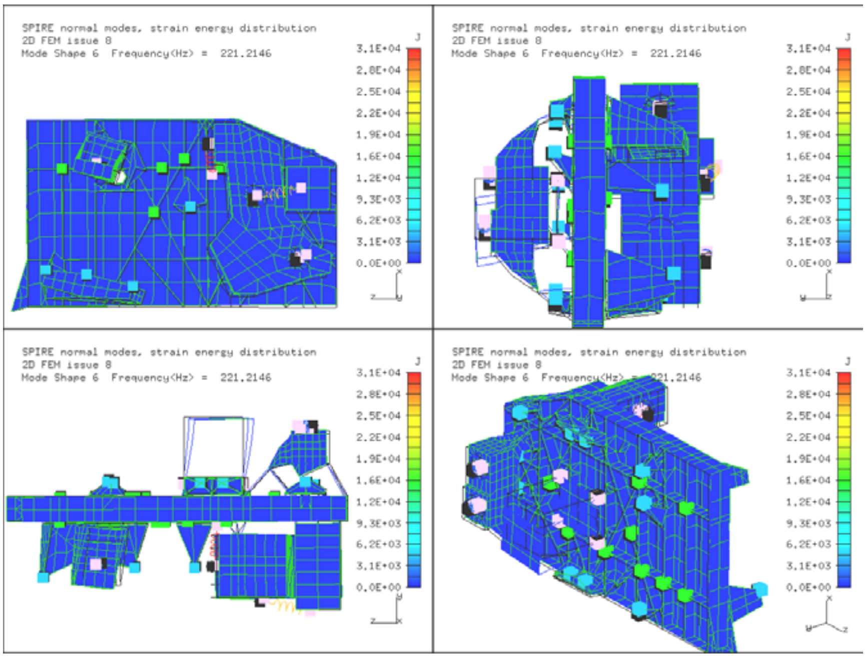
SPIRE normal modes, strain energy distribution
2D FEM issue 8
Mode Shape 6 Frequency(Hz) = 221.2146
J
3.1E+04
2.8E+04
2.5E+04
2.2E+04
1.9E+04
1.6E+04
1.2E+04
9.3E+03
6.2E+03
3.1E+03
0.0E+00

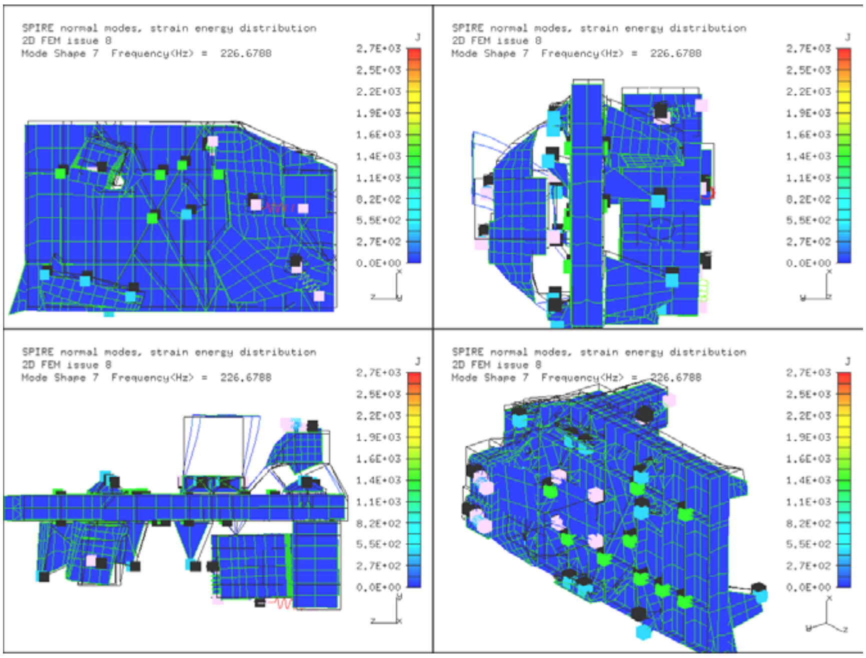
SPIRE normal modes, strain energy distribution
2D FEM issue 8
Mode Shape 7 Frequency(Hz) = 226.6788
J
2.7E+03
2.5E+03
2.2E+03
1.9E+03
1.6E+03
1.4E+03
1.1E+03
8.2E+02
5.5E+02
2.7E+02
0.0E+00

Mode 7

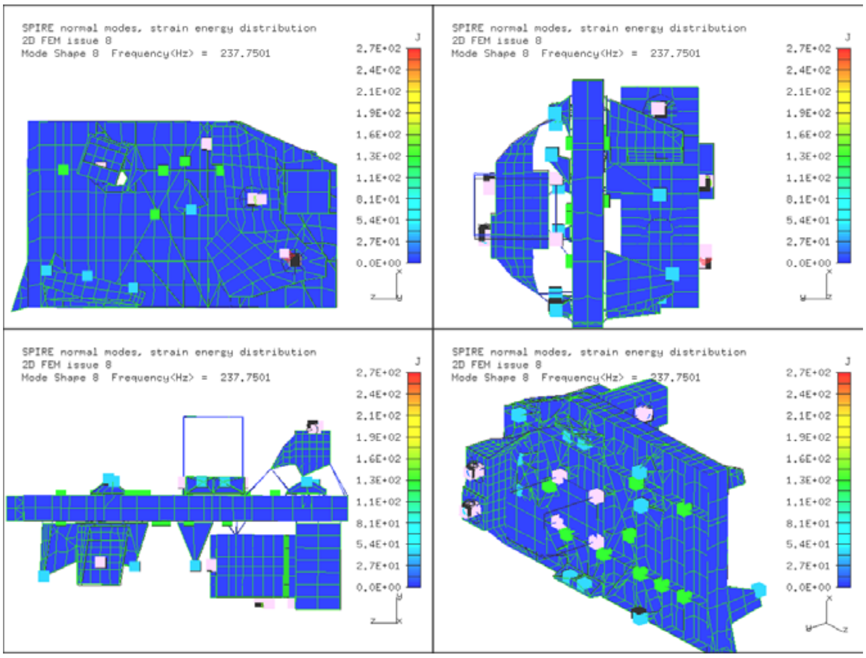
SPIRE normal modes, strain energy distribution
2D FEM issue 8
Mode Shape 8 Frequency(Hz) = 237.7501
J
2.7E+02
2.4E+02
2.1E+02
1.9E+02
1.6E+02
1.3E+02
1.1E+02
8.1E+01
5.4E+01
2.7E+01
0.0E+00

Mode 8

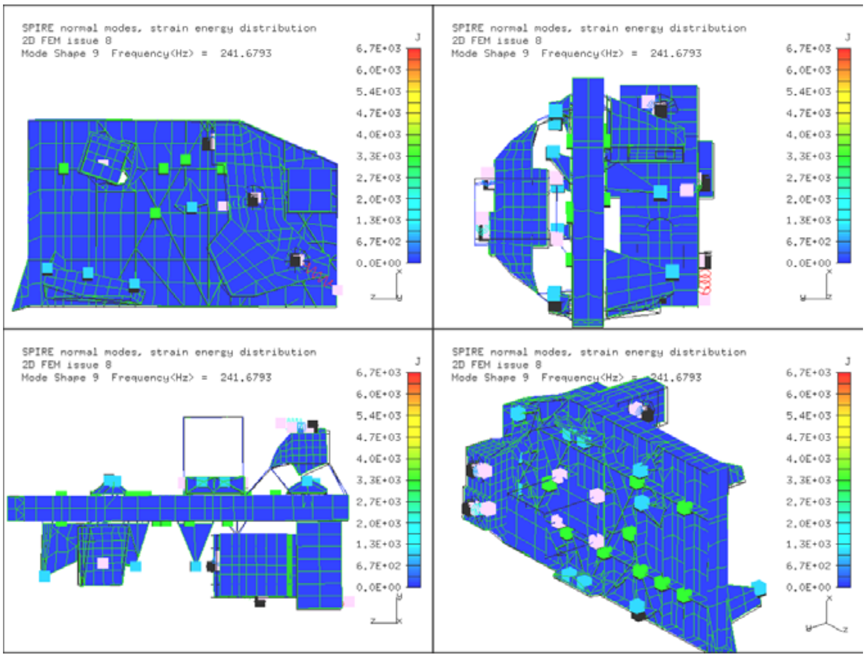
SPIRE normal modes, strain energy distribution
2D FEM issue 8
Mode Shape 9 Frequency(Hz) = 241.6793
J
6.7E+03
6.0E+03
5.4E+03
4.7E+03
4.0E+03
3.3E+03
2.7E+03
2.0E+03
1.3E+03
6.7E+02
0.0E+00
SPIRE normal modes, strain energy distribution
2D FEM issue 8
Mode Shape 9 Frequency(Hz) = 241.6793
J
6.7E+03
6.0E+03
5.4E+03
4.7E+03
4.0E+03
3.3E+03
2.7E+03
2.0E+03
1.3E+03
6.7E+02
0.0E+00
SPIRE normal modes, strain energy distribution
2D FEM issue 8
Mode Shape 9 Frequency(Hz) = 241.6793
J
6.7E+03
6.0E+03
5.4E+03
4.7E+03
4.0E+03
3.3E+03
2.7E+03
2.0E+03
1.3E+03
6.7E+02
0.0E+00
SPIRE normal modes, strain energy distribution
2D FEM issue 8
Mode Shape 9 Frequency(Hz) = 241.6793
J
6.7E+03
6.0E+03
5.4E+03
4.7E+03
4.0E+03
3.3E+03
2.7E+03
2.0E+03
1.3E+03
6.7E+02
0.0E+00

Mode 9